# Third-harmonic generation and multiphoton ionization in Bessel beams

V. E. Peet and R. V. Tsubin*
*Institute of Physics, Riia 142, Tartu EE2400, Estonia*
(Received 10 March 1997)

Three-photon resonance enhancement of third-harmonic generation and multiphoton ionization have been studied in xenon under excitation by the Bessel and the focused annular laser beams. It has been shown that the transformation of a Gaussian beam into a Bessel or an annular one leads to significant changes of third-harmonic excitation profiles and ionization spectra. These changes result from a principal difference of the beams, where either collinear (Gaussian beams) or noncollinear (Bessel and focused annular beams) excitation geometries are realized. It has been shown that the noncollinear ring-type phase matching shifts the maximum of the generated third harmonic to the longer wavelength toward the atomic resonance. Numerical calculations of third-harmonic excitation spectra have been carried out and compared with experimental results. The efficiency of frequency tripling in collinear and noncollinear excitation geometries have been compared. Cancellation of the three-photon $6s$ resonance and the influence of harmonic photons on the excitation of the four-photon $4f$ resonance in the Bessel beams are discussed. [S1050-2947(97)06508-6]

PACS number(s): 42.65.Ky, 32.80.Rm

## I. INTRODUCTION

Frequency tripling of the fundamental laser light is a well-known phenomenon of nonlinear optics. Third-harmonic (TH) generation in gases has long been established as a method for the generation of coherent UV and VUV radiation. For intense laser beams the process of TH generation is accompanied by the multiphoton ionization of gas atoms. It changes the properties of the gaseous medium and the onset of intense ionization is one of the limiting factors for tripling efficiency. On the other hand, gas-phase multiphoton ionization and resonance-enhanced multiphoton ionization (REMPI) are effective and widespread techniques of laser spectroscopy. A large number of experimental and theoretical works on REMPI have shown the importance of the harmonics of the fundamental laser light in the response of atomic system under excitation (see, e.g., [1–10], and references therein).

In recent years the generation, properties, and interaction with matter of new types of non-Gaussian and modified Gaussian laser beams have been of great interest. So-called ''diffraction-free'' Bessel beams, introduced by Durnin and co-workers [11], show a number of interesting effects in the field of nonlinear optics [12–16]. Due to a sharp intensity peak and an extended excitation region the zero-order Bessel beams are able to induce a variety of nonlinear effects, but in many cases these effects are manifested with significant differences as compared with the ordinary Gaussian beams. The differences result from the principal difference between the Gaussian and the Bessel beams. In the beam waist of a Gaussian beam the nonlinear processes are driven in a collinear excitation geometry. The Bessel beams, in contrast, realize noncollinear geometry and the cone angle of the Bessel beam serves as an additional tunable parameter [13,15,16].

There is another way to realize noncollinear excitation geometry. A Gaussian beam can be transformed into an annular one, where the intensity distribution has the form of a ring. A focused annular beam forms a cone of waves like a Bessel beam and the intensity profile in the focal spot of an annular beam is very similar to the central part of a Bessel beam. Recently it has been shown that the annular beams provide an efficient generation of TH due to self-organized ring-type phase matching [17]. A theory of this self-phase-matching (SPM) phenomenon has been developed in [18,19], where the conical beam was considered as a superposition of the Bessel beams.

Frequency tripling in SPM geometry was studied in [17] for the fixed laser wavelength and the phase matching was achieved by changing atomic vapor density. This experimental situation was treated in theoretical works on SPM [18,19]. Several specific effects of SPM geometry were observed in REMPI experiments [20,21], where a tunable dye laser was used and both the gas pressure and the laser wavelength were variable parameters for the phase matching. In those experiments, however, the TH photons were not detected directly but through the appearance of additional ionization pathways. Therefore, there are still a number of questions concerning the efficiency of tunable TH generation in SPM geometry, the role of harmonic photons in REMPI, the tuning range of resonance-enhanced TH, the influence of different geometrical factors (focusing angle, the length of the Bessel beam, geometry of an annular beam), and others. In the present paper, we report experimental observations and numerical analysis of some of these topics.

## II. EXPERIMENT

In experiments both the resonance-enhanced TH and REMPI were measured with the aid of the experimental apparatus shown schematically in Fig. 1. The output of an excimer-pumped tunable dye laser was focused into a static gas cell. The cell was made of stainless steel and contained xenon at pressures ranging from 1 to 1500 mbar. The dye

*Also at Department of Physics and Chemistry, University of Tartu, Tähe 4, Tartu EE2400, Estonia.

 

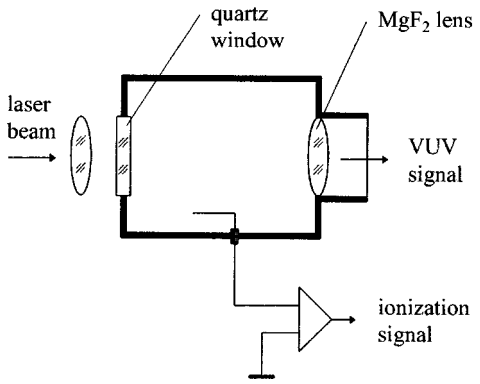


FIG. 1. Schematic diagram of the experimental apparatus.

laser was operated in the 430–442-nm spectral range (Coumarin-120 dye) and the laser pulses had an energy of 1–2 mJ, a pulse duration of 8–10 ns, and a spectral width of 0.01 nm full width at half maximum.

Photoelectrons resulting from the multiphoton ionization process were monitored with a wire collector biased at +15 V. The ionization signal was amplified, digitized by a 12-bit analog-to-digital converter, and stored on a computer. The VUV emission of TH was collected by an $f=20$ mm $MgF_2$ lens and directed onto the entrance slit of the VUV monochromator. The VUV signal was measured by a solar-blind photomultipler. This signal was amplified by a charge-sensitive radiometer, digitized, and stored on computer. In some experiments the TH generation was registered by the ionization method similar to that used in [2,22]. In this case a tantalum foil was placed behind the $MgF_2$ lens and the signal of ejected photoelectrons was measured.

Figure 2 shows different excitation configurations used in experiments. The Bessel beam was produced by a quartz

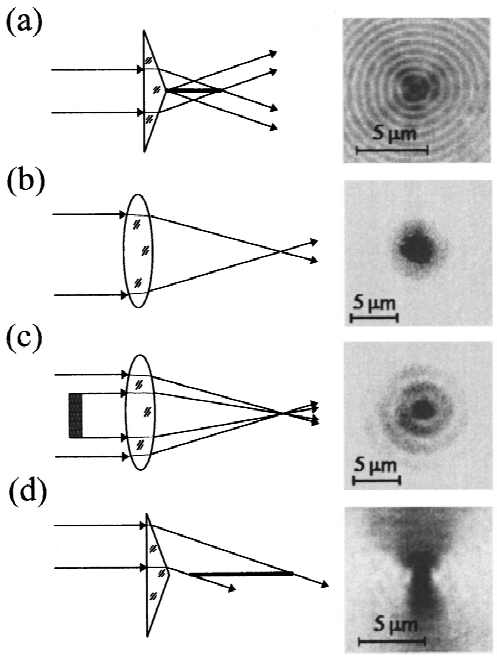


FIG. 2. Focusing geometries and the focal spots of the used laser beams: (a) Bessel beam, (b) Gaussian beam, (c) annular beam, (d) off-axis beam. CCD pictures are shown negative with an enhanced contrast.

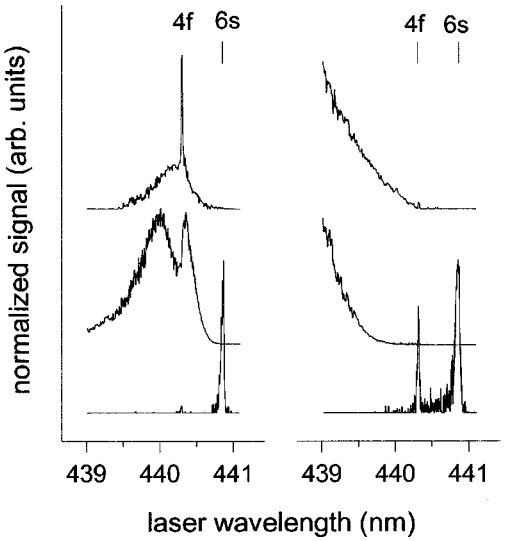


FIG. 3. Wavelength scans of REMPI and TH signals. Left column: xenon pressure 20 mbar; right column: 100 mbar. From top to bottom: ionization signal for the Gaussian beam; TH output for the Gaussian beam; ionization signal for the Bessel beam.

axicon [Fig. 2(a)], which was mounted as an input window of the gas cell. The axicon had the cone angle of 120° and the produced Bessel beam had an inclination angle of 17°. In experiments with counterpropagating Bessel beams a pair of identical axicons was used, where the second reflective axicon was mounted inside the gas cell (see Fig. 3 in Ref. [20]).

The amplitude profile of the dye laser beam was close to a Gaussian one. The beam was focused via a quartz window into the gas cell by an $f=35$ mm lens (Fig. 1) and the produced focused Gaussian beam [Fig. 2(b)] had a confocal parameter $b$ of about 100 $\mu$m. The annular beam [Fig. 2(c)] was formed with the aid of an iris diaphragm and a central mask. We used a fixed geometry of the annular beam, which had inner and the outer diameters of 3 mm and 5 mm, respectively. The same $f=35$ mm lens was used to focus the annular beam into the cell. In some experiments with axicon the laser beam was shifted off the axicon's axis [Fig. 2(d)]. Such an off-axis beam was focused by the axicon into a thin focal line, which was twice as long as for the on-axis geometry.

Figure 2 shows also the spatial distributions of light intensity in the focal regions of the beams used. The focal spots were projected by a microscope and the magnified images were recorded by a charge-coupled device (CCD) camera DIC-HR (World Precision Instruments). The maximum light intensity in the beam waist of the Gaussian beam was of the order of $10^{10}$ W/cm$^2$. For the annular beam used the measured intensity was about two times lower than for the initial Gaussian beam of the same pulse energy. This ratio agrees well with the calculation results of [23], where the same geometry of the annular beams has been considered. In the Bessel beams the light intensity was by at least an order of magnitude lower than in the Gaussian beam.

## III. RESULTS AND DISCUSSION

Both REMPI and tunable TH generation were studied near the three-photon 6$s$ resonance of xenon. The general

picture of the excitation processes for this system has been well studied in a broad range of excitation conditions [1–8,24]. For a Gaussian beam the ionization signal at a moderate xenon pressure closely follows the TH excitation profile. An example of simultaneously recorded REMPI spectra and TH is shown in Fig. 3. For the xenon pressures used the three-photon $6s$ resonance in ionization spectra is absent as a result of the well-known cancellation effect (see, e.g., [3–6]). Resonance-enhanced TH with a pressure-dependent excitation profile is generated near the $6s$ resonance. When TH overlaps the four-photon $4f$ resonances, a distinct reabsorption dip appears on the TH excitation profile (Fig. 3). In REMPI spectra it results in an intense ionization peak at the resonance position. Further increase of pressure shifts TH off the $4f$ resonance and the $4f$ peak is deenhanced. The ionization signal continues to follow the TH excitation profile, but resonance ionization near the $4f$ is suppressed. Such interplay between the TH generation and resonance ionization has been studied in several works [1,5,7,8] and our experiments with the Gaussian beams have shown similar results.

Ionization spectra undergo significant changes when the laser beam is focused by the axicon (Fig. 3). For the Bessel beam a prominent ionization peak appears very close to the $6s$ resonance. Instead of an intense $4f$ resonance a weak peak is registered at 20 mbar for the Bessel beam. At an increased xenon pressure the situation is inverted and an intense $4f$ resonance is developed for the Bessel beam, whereas a very weak peak, if any, can be registered with the Gaussian beam.

The peak near the $6s$ resonance is similar to an intense ionization band registered in high-pressure ionization experiments with the Bessel beams [20]. That band was produced by TH photons, generated in conditions of SPM [20]. Keeping in mind such an intense ionization feature, an efficient TH generation could be expected for the Bessel beams. However, all the attempts to detect the VUV emission from the cell failed if the axicon was used to focus the laser beam. For comparison, for the Gaussian and the focused annular beams the VUV signal was very intense and TH emission could easily be measured even by a simple ionization cell. The absence of VUV signal did not allow us to carry out direct measurements of TH excitation profiles for the Bessel beams. Such information has been obtained from the ionization spectra and from experiments with the annular beams.

One of the reasons why the VUV emission was not detected in the Bessel beams is obvious: an increased interaction length of a Bessel beam is obtained at the expense of power. An axicon gives a maximum light intensity 1–2 orders of magnitude lower than the corresponding spherical lens [25]. It reduces the tripling efficiency because of the $I^3$ power dependence for the TH generation. Another reason is reabsorption of the TH. As will be discussed below, for a tightly focused Bessel beam the maximum of generated TH is always located very close to the atomic resonance. In this region the absorption of TH photons is very strong. This absorption produces an intense resonance-enhanced ionization but no measurable VUV light exits the gas cell.

Figure 4 shows the evolution of ionization spectra with xenon pressure. These spectra were measured with the Bessel beams in two excitation geometries: in the common

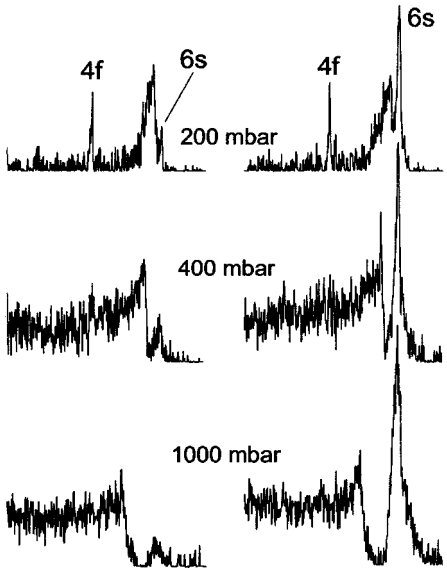


FIG. 4. REMPI spectra at different xenon pressures: left column: unidirectional Bessel beam; right column: counterpropagating Bessel beams.

unidirectional one and in counterpropagating Bessel beams. With an increased gas pressure the ionization band shifts off the atomic resonance and a distinct long tail is developed on the band toward the shorter wavelength. From the long-wavelength side the band has a sharp cutoff and a gap arises between the atomic peak and the band. A remarkable feature of the spectra for unidirectional Bessel beam is the presence of a quite intense ionization signal at the position of the $6s$ resonance. A similar effect was observed in high-pressure ionization experiments, where the $6s$ resonance could be seen at a pressure of several bars [20]. These observations are in a sharp contrast with the case of the Gaussian beams, where the three-photon $6s$ resonance vanishes for xenon pressure above a few mbar. We will come back later to this remarkable point.

The use of counterpropagating beams is a common tool to observe the canceled resonances. In this case the coherent field at the sum frequency is not able to suppress the resonance ionization, as the laser photons have two traveling directions and no sum-frequency field is generated when the photons are absorbed from the opposite beams. As a result, in counterpropagating Bessel beams an intense $6s$ resonance appears in the spectra. Besides, in counterpropagating beams the TH generation is suppressed. It leads to suppression of the corresponding ionization band near resonance [20]. In the case here, however, such suppression was not well pronounced. The reason for this is very simple. The experiments with counterpropagating beams are extremely sensitive to the overlap of the beams and in real experimental conditions the beams are far from being completely overlapped. In laser-induced breakdown experiments [20] the optical signal of plasma emission came out of the spatial regions with maximum light intensity, i.e., the regions with a good overlap of the beams. In the present experiments there was no such spatial selection and a reduced ionization in the overlapped parts of the beams was covered by the total ionization signal from the individual beams.

In order to consider the generation of TH in the Bessel

beams we applied the theory of SPM developed for conical beams [18,19]. In a simplified manner the results of [18,19] have been used in [20,21], where the spectral width and the position of TH maximum have been calculated. The goal of the present numerical work was to get the spectral dependence of the tunable TH generation and to compare the calculation results with experimental observations.

The intensity of the TH field is given by the expression [18,19]

$$|E_3|^2 = 2\pi \int |\psi_3^+|^2 \rho d\rho, \tag{1}$$

where the amplitude of the generated TH

$$\psi_3^+ \sim \frac{\omega_3^2}{k_3} \chi^{(3)}(\omega_1,\omega_1,\omega_1) \tan\beta \left(\frac{\sin\theta}{\theta}\right) I J_0(k_3 \sin\beta\rho), \tag{2}$$

$$\theta = \frac{L}{2}(k_3\cos\beta - 3k_1\cos\alpha), \tag{3}$$

$$I = 2\pi \int_0^\infty \rho J_0(k_3\sin\beta\rho)[J_0(k_1\sin\alpha\rho)]^3 d\rho. \tag{4}$$

Here $\chi^{(3)}(\omega_1,\omega_1,\omega_1,)$ is the nonlinear susceptibility for TH generation, $\rho$ is the radial coordinate, $L$ is the length of the medium, $\alpha(\beta)$, $k_1(k_3)$, and $\omega_1(\omega_3)$ are the inclination angle, the wave vector, and the angular frequency of the fundamental (TH) light, respectively. In expression (2) we leave out some terms that are independent on the wavelength.

In our numerical calculations we made a simplification with the treatment of the Bessel functions. In experiments the Bessel beams are realized within a finite aperture. Therefore, the $J_0$ amplitude profile is actual for some limited spatial volume but vanishes elsewhere. This feature is even more enhanced in a nonlinear optical process, where the main contribution comes from the central part of the beam with maximum light intensity. It allows one to treat the fundamental beam as a Bessel-Gauss beam [26] rather than a Bessel one. For a Bessel-Gauss beam the function $J_0$ is multiplied by the Gaussian term $\exp[-(\rho/w)^2]$. This term suppresses outer oscillations of $J_0$ but, at a proper choice of $w$, makes no essential influence at small $\rho$. Such an approach simplifies the treatment of the transverse-phase-matching integral (4), as for the Bessel-Gauss beam the integral can be solved over a finite volume without oscillations of solution. Besides, it eliminates the divergence of the integral (4) at $T=1$, where $T=(k_3\sin\beta)/(k_1\sin\alpha)$ [18,19]. In our calculations the integration was carried over the first 20 rings of the fundamental beam and the parameter $w$ was arbitrarily chosen to suppress the 20th maximum of $|J_0|$ below 0.01 of its value. For the TH beam we did not apply the Bessel-Gauss representation and it was treated as a Bessel one. For the nonlinear susceptibility $\chi^{(3)}$ we used the calculation results of [27] and only the resonant part of $\chi^{(3)}$ was taken into account. The refraction indices for the fundamental beam and for the TH light were calculated by using the Sellmeir formula and the data of [28] about the oscillator strengths for xenon transitions.

Curve 1 in Fig. 5 shows the TH excitation profile calculated for the Bessel beam. This curve represents the result of direct numerical treatment of Eqs. (1)–(4) without any fitting parameter. A close similarity of the calculated curve and the ionization peaks in REMPI spectra (Figs. 3 and 4) is obvious. The calculated dependence of TH generation reproduces well the sharp maximum near the atomic resonance, the long tail toward the shorter wavelength and the cutoff at the red edge.

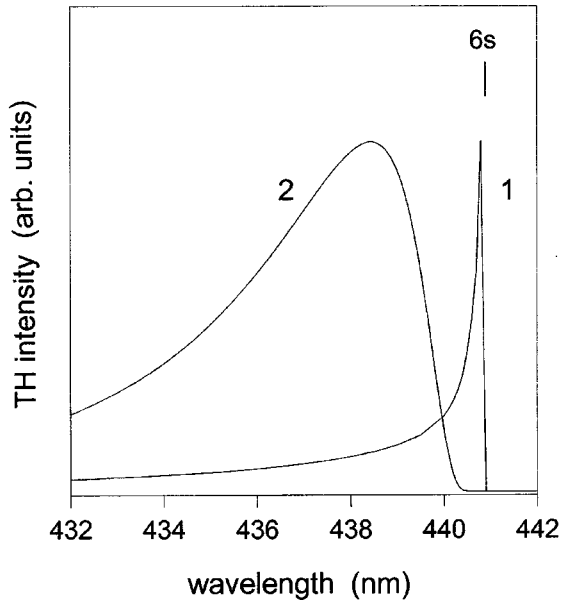


FIG. 5. Calculated spectral dependences of the TH generation. 1: Bessel beam with $\alpha = 17°$; 2: Gaussian beam with $b = 100$ $\mu$m. Xenon pressure 50 mbar.

The maximum of TH corresponds to the maximum spatial overlap of the cube of the fundamental Bessel beam with the Bessel beam of generated TH. In this case $T=1$ and the cone of TH light has the inclination angle $\beta_0$ given by [18,19]

$$\tan(\beta_0) = \tfrac{1}{3}\tan(\alpha). \tag{5}$$

In our case $\beta_0 = 5.8°$. The long tail of the TH tuning curve corresponds to $1<T<3$ and in this region $\beta_0<\beta<\alpha$. Near the long-wavelength edge $0<T<1$ and $0<\beta<\beta_0$.

For comparison, Fig. 5 shows the TH excitation profile calculated for the Gaussian beam with the confocal parameter $b = 100$ $\mu$m. This dependence was obtained by numerical calculation of the well-known phase-matching integral for a tightly focused Gaussian beam [29]

$$|F(b\Delta k)|^2 = \begin{cases} \pi^2 (b\Delta k)^2 \exp(b\Delta k), & \Delta k < 0 \\ 0, & \Delta k > 0, \end{cases} \tag{6}$$

where $\Delta k = k_3 - 3k_1$. It is interesting to note that for the Bessel beam the spectral dependence of TH can be quite well reproduced by the phase-matching integral (6) if an extremely short (3–4 $\mu$m) confocal parameter $b$ is assumed. In this case the calculated curve shows a very similar sharp peak near the resonance but without a long tail. It is difficult to say whether such a formal similarity has some physical background. At least, it may be useful for a qualitative com-

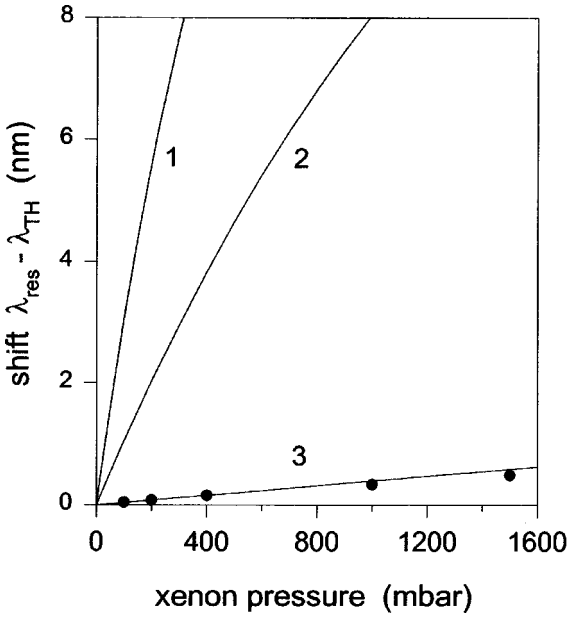


FIG. 6. Calculated shift of the TH maximum with pressure. 1: Gaussian beam with $b=100$ $\mu$m; 2: Bessel beam with $\alpha=3.3°$; 3: Bessel beam with $\alpha=17°$. Full circles show the measured positions of the TH ionization peak in REMPI spectra.

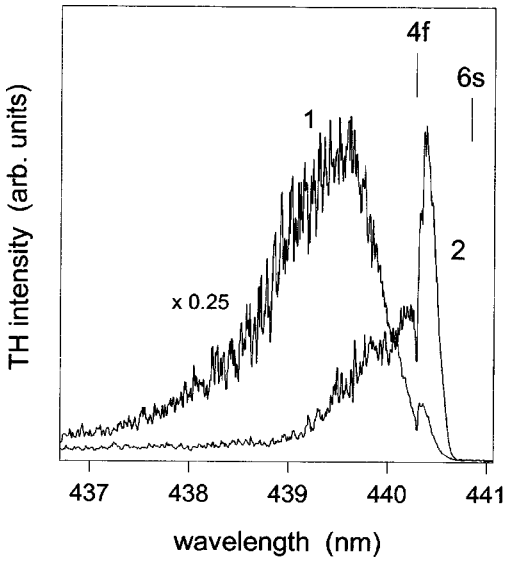


FIG. 7. Spectral dependences of the TH output. 1: Gaussian beam; 2: annular beam. Xenon pressure 50 mbar.

parison of nonlinear optical effects in the Gaussian and in the Bessel beams. Below we show some examples of such comparison.

Figure 6 shows the calculated shift of the TH maximum from the 6$s$ resonance as a function of xenon pressure. For a tightly focused Gaussian beam the maximum of TH is achieved at $b\Delta k=-2$ and with an increased gas pressure the maximum shifts rapidly off the resonance (curve 1 in Fig. 6). For the Bessel beams (curves 2 and 3 in Fig. 6) the position of the TH maximum shows larger tolerance against the pressure and for the beam with $\alpha=17°$ the TH bands remain in the vicinity of the atomic resonance for the whole pressure range. Note the good agreement of the calculated dependence 3 in Fig. 6 and the data of present experiments. In high-pressure experiments [20] a shift of 0.26 nm/bar for the ionization band has been reported and it agrees well with the slope of 0.3 nm/bar for the curve 3 in Fig. 6.

Extremely different pressure dependences reflect the different phase-matching conditions for the TH generation, which are realized in the Bessel and the Gaussian beams. For a Bessel beam the SPM phenomenon compensates large variations of the refractive index. It makes it possible to produce tunable TH in a more broad range of excitation wavelength and gas pressure as compared with the Gaussian beams [20,21]. However, there are other important factors that can spoil such a formal advantage of the Bessel beams for frequency tripling. For a Gaussian beam the phase-matching curve rapidly shifts off the atomic resonance with an increased gas pressure. For some pressure range it preserves relatively high TH efficiency, as due to the pressure-induced shift the maximum of generated TH avoids an increased absorption near the atomic resonance. In contrast, for a tightly focused Bessel beam the maximum of TH is always located near the atomic resonance, where the absorption of TH photons is very strong. For the excitation wavelength far enough from the resonance the efficiency of TH generation is much lower (the tail of the TH excitation spectrum). To shift the maximum of TH off the resonance the inclination angle $\alpha$ must be reduced. Such Bessel beams, however, lose intensity because of an increased excitation length. In this case the $I^3$ power dependence will lead to a significant decrease of efficiency in spite of reduced TH reabsorption. Thus, for the Bessel beams two contradictory conditions are encountered. To get a high light intensity the beams with large $\alpha$ should be used, whereas small angles $\alpha$ are required to avoid the reabsorption of TH. In this sense, for the Bessel beams the generated TH field is to be considered mainly as an internal one. The TH photons are generated and they participate in a variety of excitation and ionization processes, but the output of TH light is very weak.

Focused annular beams provide noncollinear excitation geometry like the Bessel beams but with much higher light intensity. Therefore, using annular beams seems to be a more efficient method of frequency tripling in SPM geometry. Figure 7 shows the spectral dependences of the TH output measured with the Gaussian and the annular laser beams. In both cases the laser pulse energy was kept constant and the loss of energy for the annular beam was compensated by attenuating the dye laser output in the measurements with the Gaussian beam. Again, as it was observed with the Bessel beams, the SPM geometry shifts the TH excitation profile toward the longer wavelength and the maximum of generated TH is achieved closer to the atomic resonance. As a result, within some spectral range the VUV output for the annular beam exceeds that for the Gaussian beam. This observation agrees with the results of [17], where the efficiency of TH generation was increased by 4–5 times when a ring-shaped beam was used instead of a disk-shaped one. Note that the experiments in [17] were carried out at a fixed laser wavelength, where the shift of TH excitation profile can give a significant rise of efficiency.

The maximum of TH generation for a Gaussian and an annular beam is achieved at different wavelengths and with different conversion efficiencies. In our case the maximum VUV output for the Gaussian beam was four times higher

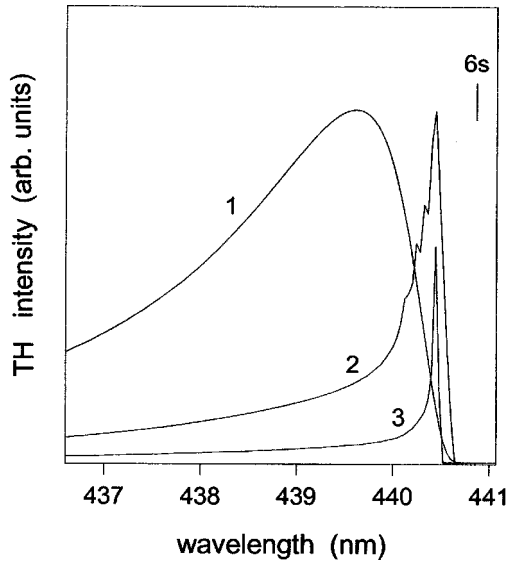


FIG. 8. Numerical simulation of experimental TH dependences in Fig. 7. 1: Gaussian beam; 2: annular beam as a superposition of ten Bessel beams; 3: single Bessel beam ($\alpha = 3.3°$).

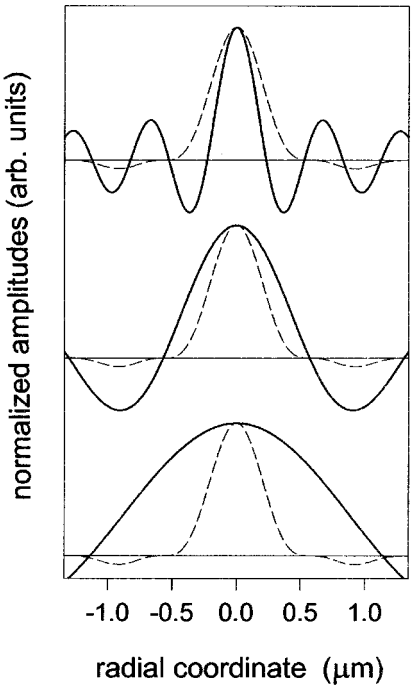


FIG. 9. Normalized spatial distributions of the amplitudes $E_3$ (solid lines) and $E_1^3$ (dashed lines). From top to bottom: $\beta = 14°$; $\beta = \beta_0 = 5.8°$; $\beta = 3°$. Wavelength of the fundamental Bessel beam $\lambda = 440$ nm, inclination angle $\alpha = 17°$.

than that for the annular beam of the same energy. Such an advantage of the Gaussian beam comes mainly from a good focusability of these beams and a high power density in their beam waist. For the annular beam used the light intensity was about two times lower than in the corresponding Gaussian beam. Thus, being normalized in light intensity and taking into account the $I^3$ dependence, the efficiency of the annular beam is, actually, about two times higher.

Experimental dependences in Fig. 7 were simulated by numerical calculations of the TH generation. Again, the theory of SPM [18,19] was applied, where the annular beam was treated as a set of thin-ring slits [19]. Every slit produces an individual Bessel beam and these Bessel beams overlap in the nonlinear medium. The generated TH photons come from all combinations of the three photons of the fundamental beams. The output TH radiation results from a superposition of multiple Bessel beams with different angles $\beta$. We calculated the TH output as a superposition of ten Bessel beams. Such an approach corresponds to an annular beam, represented by three ring slits [19].

Figure 8 shows the calculated phase-matching curves for the Gaussian beam with $b = 100$ $\mu$m, for the annular beam and for a single Bessel beam. The last corresponds to a single ring slit having mean diameter of the annular beam $d_m = 4$ mm ($\alpha = 3.3°$). For this single Bessel beam the position of the TH maximum coincides with that registered in experiments, but the calculated TH excitation profile is too sharp and narrow. Superposition of multiple Bessel beams increases the width of the TH profile and the calculated curve reproduces much better the shape of the experimental spectral dependence. With an increased gas pressure the spectral distance between the TH maxima for the annular and the Gaussian beams increases, as can be seen from Fig. 6 (curves 1 and 2). Note again that the TH output for the annular beam can be quite well approximated by the phase-matching integral (6). In the case here, the phase-matching curve 2 in Fig. 8 formally corresponds to that for the initial Gaussian beams (curve 1) but with $b$ reduced by 5–6 times.

As mentioned above, for the Bessel beams the three-photon 6$s$ resonance in REMPI spectra is partially canceled but, in sharp contrast to the Gaussian beams, the residual uncanceled peak is always quite intense. This remarkable difference between the Bessel and the Gaussian beams results from spatial effects in TH generation. The cancellation of resonant ionization is caused by destructive interference between the three- and the one-photon excitation processes, where the one-photon process is driven by the TH field. A complete suppression of resonant ionization occurs if the cancellation effect works point by point everywhere within the excitation volume. For the amplitudes of interacting fields it means that the TH field $E_3$ and the cube of the fundamental field $E_1^3$ should have the same spatial distributions. In this case the interference between the three-photon excitation process (driven by $E_1^3$) and the one-photon process (driven by $E_3$) is able to cancel resonant ionization in any point of the excitation volume. Apart from some propagation effects [24] such a situation is realized for the beam waist of a Gaussian beam, where the transverse profiles of $E_1^3$ and $E_3$ coincide.

For the Bessel beams both the fundamental and the TH fields have $J_0$ amplitude profiles and the spatial periods of these oscillating functions are, in general, different. This is illustrated in Fig. 9, where the spatial distributions of $E_1^3$ and $E_3$ are shown for the fundamental beam with $\alpha = 17°$ and the TH beams with three different values of $\beta$. Certainly, large absorption of on-resonance TH transforms the profiles of $E_3$, but for demonstration purposes it can be neglected. Even at $\beta = \beta_0$ the profiles of $E_1^3$ and $E_3$ differ and this difference is even more enhanced for $\beta > \beta_0$ and $\beta < \beta_0$. Therefore, for a Bessel beam there are always some spatial regions near the beam axis, where $E_1^3$ is close to zero but $E_3$ is nonzero and

vice versa. In these regions the cancellation is spoiled and either $E_1^3$ drives the three-photon transitions or $E_3$ drives the one-photon transitions. It is clear that the total ionization signal, integrated over all values of $\beta$ and over the whole excitation volume, will show an uncanceled peak at the resonance position.

We will now consider the effects of generated TH on the excitation of the four-photon $4f$ resonances. For a Gaussian beam the $4f$ peak in REMPI spectra is enhanced when the TH overlaps these resonances. In this case a dip appears on the TH profiles (Figs. 3 and 7). When the TH band is shifted to the shorter wavelength, the cancellation occurs and the $4f$ peak is deenhanced (Fig. 3). This cancellation can be considered in terms of an off-resonance destructive interference, which interrupts the excitation pathway to the $4f$ states [7,8,27].

For the Bessel beam the $4f$ peak shows similar behavior. Starting from some pressure the peak is enhanced and it disappears with an increased pressure (Figs. 3 and 4). Note, however, that the pressure necessary to enhance or to suppress the resonance is much higher than in the case of the Gaussian beam. Besides, for a Gaussian beam the cancellation occurs at a smaller detuning from the $6s$ resonance than that of maximum TH [27]. This means that to cancel the $4f$ peak the gas pressure must be high enough to shift the TH tuning range off the $4f$ resonances. For the Bessel beam the TH excitation band is always located near the $6s$ resonance. Therefore, for any pressure the $4f$ resonance is overlapped by the tail of the TH phase-matching curve and the cancellation occurs without the shift of TH off the $4f$ resonance.

For a Gaussian beam the pressure condition for cancellation to work can be written as [27]

$$|\mathrm{Im}(\Delta k)|b \gg 1. \tag{7}$$

The condition (7) means that the cancellation occurs when the absorption length for the TH light is much smaller than the length of the excitation region. As mentioned above, the spectral dependence of the TH generation in a Bessel beam corresponds formally to that for a Gaussian beam having very small $b$. Such formal similarity explains qualitatively the need of higher gas pressure to cancel the $4f$ peak in a Bessel beam. For an extremely small $b$ the pressure condition (7) requires very short absorption length, i.e., a high gas density. Again, it is difficult to say whether such an approach is correct, though it explains qualitatively the large difference in pressures necessary to cancel the $4f$ resonance.

Interesting transformations of REMPI spectra were observed in experiments where the laser beam was focused by axicon. Within some pressure range the main spectral features were very sensitive to the position of the laser beam on the axicon. This is illustrated in Fig. 10, where the wavelength scans of the REMPI signal are shown for on- and off-axis excitation geometries. If the laser beam is centered on the axicon, the Bessel beam is produced and the TH peak is the most intensive one. When the beam is shifted on the axicon, the TH peak is gradually reduced and vanishes under off-axis excitation. On the contrary, the $4f$ peak increases and it is the most intensive one under off-axis excitation.

For an off-axis excitation geometry the cone of the fundamental Bessel beam disappears, as the off-axis beam produces only a part of this cone. Therefore, there are no combinations of the wave vectors to generate TH near the atomic resonance and the TH peak in the REMPI spectrum disappears. Nevertheless, the TH light still can be produced in other spectral regions and, probably, this causes an enhancement of the $4f$ peak. The off-axis beam behind the axicon has a new propagation direction, which is inclined by the angle $\alpha$ with respect to the initial beam. It is easy to see from simple geometrical consideration that the maximum inclination angle for the wave vectors in the refracted beam is $\alpha^* = (d/2h)\alpha$, where $d$ is beam diameter and $h$ is the distance between the axes of the beam and the axicon. For an off-axis excitation geometry $(d/2h) < 1$, therefore $\alpha^* < \alpha$. Reduced inclination angle shifts the maximum and the tuning range of TH to the shorter wavelength, where generated TH photons enhance resonance ionization via the $4f$ states.

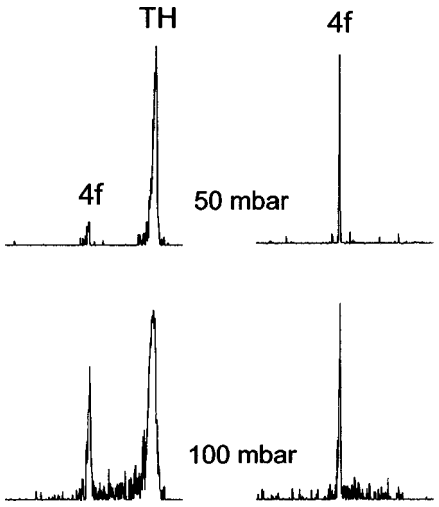


FIG. 10. Wavelength scans of the ionization signal: left column: on-axis excitation (Bessel beam); right column: off-axis excitation.

## IV. CONCLUSION

Three-photon resonance-enhanced TH generation and REMPI of xenon in the Bessel and the focused annular beams show several specific features as compared with the case of the ordinary Gaussian laser beams. For the Bessel and the annular beam the nonlinear optical processes are driven in a noncollinear excitation geometry. In this case the TH generation proceeds in ring-type SPM conditions. The experiments have shown that the SPM expands the TH tuning range toward the three-photon atomic resonance and the maximum of generated TH is achieved closer to this resonance. For the Bessel beams it leads to the appearance of an intense ionization band near the resonance. However, the generated TH for the Bessel beams is to be considered mainly as an internal one, as the output of VUV emission from the tripling cell is very weak. The low yield of TH is caused by reabsorption of the VUV photons, as for a tightly focused Bessel beam the maximum of TH is always located near the atomic resonance. To shift the TH maximum off resonance the Bessel beams with small inclination angle should be used. Such beams, however, lose light intensity. In this sense, the Bessel beams are hardly competitive with the Gaussian ones in overall efficiency of frequency tripling.

Focused annular beams represent a more effective way to realize SPM geometry. It has been shown that the transformation of a Gaussian beam into an annular one shifts the maximum of generated TH to a longer wavelength. As a result, within some spectral range the TH output for an annular beam can exceed that for the initial Gaussian beam. This circumstance is important for frequency tripling at a fixed laser wavelength, where such a shift of the TH excitation profile can increase the tripling efficiency [17]. The overall efficiency can be even more enhanced by using more effective schemes to produce the annular beam. For example, a pair of refractive axicons can transform a laser beam into an annular one without loss of energy on the central mask.

Numerical simulation of the TH excitation spectra has shown a good agreement with the experimental data. In the calculations we used the theory of SPM developed in [18,19] and the fundamental Bessel beam was treated as a Bessel-Gauss one. Such an approach has proved valid and the calculation results reproduce well the ionization band in REMPI spectra, the shift of this band with pressure, and the TH excitation profiles for an annular beam.

The cancellation of the three-photon $6s$ atomic resonance in the Bessel and the Gaussian beams is pronounced in a different manner. For the Gaussian beams this resonance is canceled for xenon pressure above a few mbar. On the contrary, for a Bessel beam the REMPI spectra always show quite an intense ionization signal at the resonance position. This difference can be explained by spatial effects in the TH generation. In a Bessel beam the fundamental and the TH lights have, in general, different spatial profiles. This leads to remarkable variations of the excitation conditions and the interference between the three- and the one-photon pathways is not able to suppress resonant ionization in every point of the excitation volume.

The enhancement and the cancellation of the four-photon $4f$ resonance in the Bessel beams are manifested similarly to the case of the Gaussian beams. The main difference is a higher gas pressure necessary to observe these effects with the Bessel beams. In this sense the Bessel beam formally behaves like a Gaussian one having very short confocal parameter. The same similarity can be stated from the spectral dependences of the TH generation in the Bessel and the Gaussian beams.

## ACKNOWLEDGMENTS

The authors gratefully thank P. Lambropoulos and V. Hizhnyakov for helpful discussions and A. Kippasto for experimental assistance. This work has been supported by the Estonian Science Foundation (Grant No. 2272).

[1] J. C. Miller, R. N. Compton, M. G. Payne, and W. R. Garrett, Phys. Rev. Lett. **45**, 114 (1980).
[2] J. C. Miller and R. N. Compton, Phys. Rev. A **25**, 2056 (1982).
[3] J. H. Glownia and R. K. Sander, Phys. Rev. Lett. **49**, 21 (1982).
[4] M. G. Payne and W. R. Garrett, Phys. Rev. A **26**, 356 (1982); **28**, 3409 (1983).
[5] D. J. Jackson, J. J. Wynne, and P. H. Kes, Phys. Rev. A **28**, 781 (1983).
[6] M. G. Payne, W. R. Garrett, and W. R. Ferrell, Phys. Rev. A **34**, 1143 (1986).
[7] D. Charalambidis, X. Xing, J. Petrakis, and C. Fotakis, Phys. Rev. A **44**, R24 (1991).
[8] X. Xing, D. Charalambidis, E. Koutsourelaki, and C. Fotakis, Phys. Rev. A **47**, 2296 (1993).
[9] W. R. Garrett, S. D. Henderson, and M. G. Payne, Phys. Rev. A **35**, 5032 (1987).
[10] D. Charalambidis, J. A. D. Stockdale, and C. Fotakis, Z. Phys. D **32**, 191 (1994).
[11] J. Durnin, J. Opt. Soc. Am. A **4**, 651 (1987); J. Durnin, J. Miceli, Jr., and J. Eberly, Phys. Rev. Lett. **58**, 1499 (1987).
[12] N. E. Andreev, Y. A. Aristov, L. Y. Polonsky, and L. N. Pyatnitsky, Zh. Éksp. Teor. Fiz. **100**, 1756 (1991) [Sov. Phys. JETP **73**, 969 (1991)].
[13] T. Wulle and S. Herminghaus, Phys. Rev. Lett. **70**, 1401 (1993).
[14] I. Golub, Opt. Lett. **20**, 1847 (1995).
[15] S. Klewitz, F. Brinkmann, S. Herminghaus, and P. Leiderer, Appl. Opt. **34**, 7670 (1995).
[16] S. Klewitz, P. Leiderer, S. Herminghaus, and S. Sogomonian, Opt. Lett. **21**, 248 (1996).
[17] B. Glushko, B. Kryzhanovsky, and D. Sarkisyan, Phys. Rev. Lett. **71**, 243 (1993).
[18] Surya P. Tewari, H. Huang, and R. W. Boyd, Phys. Rev. A **51**, R2707 (1995).
[19] Surya P. Tewari, H. Huang, and R. W. Boyd, Phys. Rev. A **54**, 2314 (1996).
[20] V. E. Peet, Phys. Rev. A **53**, 3679 (1996).
[21] V. E. Peet and R. V. Tsubin, Opt. Commun. **134**, 69 (1997).
[22] J. H. Glownia and R. K. Sander, Appl. Phys. Lett. **40**, 648 (1982).
[23] J. Ojeda-Castañeda, J. C. Escalera, and M. J. Yzuel, Opt. Commun. **114**, 189 (1995).
[24] M. G. Payne, J. C. Miller, R. C. Hart, and W. R. Garrett, Phys. Rev. A **44**, 7684 (1991).
[25] V. V. Korobkin, L. Ya. Polonskii, V. P. Poponin, and L. N. Pyatnitskii, Kvantovaya Electron. (Moscow) **13**, 265 (1986) [Sov. J. Quantum Electron. **16**, 178 (1986)].
[26] F. Gori, G. Guattari, and C. Padovani, Opt. Commun. **64**, 491 (1987).
[27] M. Elk, P. Lambropoulos, and X. Tang, Phys. Rev. A **44**, R31 (1991).
[28] W. F. Chan, G. Cooper, X. Guo, G. R. Burton, and C. E. Brion, Phys. Rev. A **46**, 149 (1992).
[29] J. F. Reintjes, *Nonlinear Optical Parametric Processes in Liquids and Gases* (Academic, New York, 1984).